# NEAR-RESONANT REGIMES OF THE MOVING LOAD ON A PRE-STRESSED INCOMPRESSIBLE ELASTIC HALF-SPACE

**Askar KUDAIBERGENOV[*], Askat KUDAIBERGENOV[*], Danila PRIKAZCHIKOV[**, ***]**

[*]Faculty of Mechanics and Mathematics, Department of Mathematical and Computer Modelling, Al-Farabi Kazakh National University, 71 Al-Farabi Ave., 050040, Almaty, Kazakhstan
[**]School of Computing and Mathematics, Keele University, Keele, Staffordshire, ST5 5BG, United Kingdom
[***]Institute for Problems in Mechanical Engineering RAS, 61 Bolshoy Pr., Saint-Petersburg, 199178, Russia

askar.kudaibergenov@kaznu.kz, askat.kudaibergenov@kaznu.kz, d.prikachikov@keele.ac.uk

*received ……., revised ……., accepted …….*

**Abstract:** The paper is concerned with the analysis of the problem for a concentrated line load moving at a constant speed along the surface of a pre-stressed, incompressible, isotropic elastic half-space, within the framework of the plane-strain assumption. The focus is on the near-critical regimes, when the speed of the load is close to that of the surface wave. Both steady-state and transient regimes are considered. Implementation of the hyperbolic-elliptic asymptotic formulation for the surface wave field allows explicit approximate solution for displacement components expressed in terms of the elementary functions, highlighting the resonant nature of the surface wave. Numerical illustrations of the solutions are presented for several material models.

**Key words:** Moving load, incompressible, pre-stress, asymptotic

## 1. INTRODUCTION

Moving loads on elastic half-space have been subject of numerous investigations, motivated by important engineering applications related to ground vibrations caused by moving transport vehicles, see e.g. (Krylov, 1996; Cao et al., 2012). In the classical contribution of (Cole and Huth, 1958) a steady-state solution for an elastic half-plane subject to a moving load was obtained. It is worth mentioning that in this early paper, the resonant nature of the Rayleigh wave may already be noticed, see also (Goldstein, 1965). A substantial part of considerations for moving loads are focused on steady-state regimes, see e.g. recent results for porous anisotropic half-space by (Wang et al., 2021), study for a thermoelastic half-space with double porosity (Kumar and Vohra, 2020). We also note the papers dealing with time-harmonic moving loads, see (Lefeuve-Mesgouez et al., 2000; Sun et al., 2019) and interesting aspects of transition when surface load moves over the interface of two elastic materials, see (van Dalen et al., 2015). There are relatively few treatments of transient modes in moving load problems, including early works (Payton, 1967; Gakenheimer and Miklowitz, 1969) and also more recent contributions (de Hoop, 2002; Kaplunov et al., 2010b). It is known that analysis of transient dynamics is generally non-trivial, often requiring numerical approach, see e.g. (Bratov, 2011; Smirnov et al., 2012). We also mention active studies of moving loads on elastic structures, see e.g. a textbook (Fryba, 1999) and references therein, as well as recent works, see e.g. (Dimitrovova, 2017; Wang et al., 2020; Lu et al., 2020).

This paper relies on a recent approach to near-resonant regimes of the moving load on an elastic half-space, originating from the hyperbolic-elliptic models for surface waves, see (Kaplunov and Prikazchikov, 2017). The models contain elliptic equations associated with decay into the interior, along with hyperbolic equations on the surface governing wave propagation. This methodology has allowed a number of explicit approximate solutions of the moving load problems, see (Kaplunov et al., 2010a; Kaplunov et al., 2013; Erbaş et al., 2017; Ege et al., 2017). The advantage of this approach is related to the representation of the surface wave field in terms of a single harmonic function, providing reduction of the vector problem of elastodynamics to a scalar formulation. Recent developments in the area include incorporation of effects of anisotropy (Fu et al., 2020), a refined second-order model (Wootton et al., 2020), explicit formulations for seismic meta-surfaces in the form of array of resonators attached to the surface (Ege et al., 2018; Wootton et al., 2019), as well as formulations for surface wave on a coated half-space with non-classical boundary conditions (Kaplunov et al., 2019)

The hyperbolic-elliptic plane-strain model for surface wave on a pre-stressed incompressible elastic half-space has been derived in (Khajiyeva et al., 2018), allowing a scalar formulation for the surface wave field induced by prescribed surface stresses. In this work, we implement these results to analyze the near-critical regimes for the line force moving at a constant speed along the surface. Both steady-state and transient problems are considered. As a result, explicit expressions for the displacement field are obtained in terms of elementary functions, confirming the resonant nature of surface wave speed. In case of transient displacements, distinction between the sub-critical, super-critical and resonant regimes follows immediately from the analysis on the surface. Then, using Poisson's formula, solution is restored over the interior. Consideration of large time limit allows approximations for the components of rigid body motion. The obtained results are illustrated numerically for several material models, including the neo-Hookean, Gent, and Gent-Gent strain-energy functions.

## 2. STATEMENT OF THE PROBLEM

Consider a homogeneous incompressible elastic body with an initial state $B_0$ in the domain $X_2 \geq 0$. Under the action of a homogeneous static deformation $x_i = x_i(X_A)$, the body transforms to a finitely deformed equilibrium state $B_e$, which corresponds to a half-space $X_2 \geq 0$, and after superimposing infinitesimal time-dependent motion $u_i(x_j, t)$, it moves to the current state $B_t$ with the position vector $\bar{x}_i(X_A, t)$ given by

$$\bar{x}_i(X_A, t) = x_i(X_A) + u_i(x_j, t). \tag{1}$$

Below, the attention is drawn to the plane strain problem, for which $u_3 = 0$ and $u_1 = u_1(x_1, x_2, t)$, $u_2 = u_2(x_1, x_2, t)$, giving the following coupled equations of incremental motion

$$A_{1111}\frac{\partial^2 u_1}{\partial x_1^2} + (A_{1122} + A_{1221})\frac{\partial^2 u_2}{\partial x_1 \partial x_2} + A_{2121}\frac{\partial^2 u_1}{\partial x_2^2} - \frac{\partial p_t}{\partial x_1} = \rho\frac{\partial^2 u_1}{\partial t^2},$$

$$A_{1212}\frac{\partial^2 u_2}{\partial x_1^2} + (A_{1122} + A_{1221})\frac{\partial^2 u_1}{\partial x_1 \partial x_2} + A_{2222}\frac{\partial^2 u_2}{\partial x_2^2} - \frac{\partial p_t}{\partial x_2} = \rho\frac{\partial^2 u_2}{\partial t^2}, \tag{2}$$

where $A_{ijkl}$ are the components of the fourth order elasticity tensor (Ogden, 1984), $\rho$ is mass density, $p_t$ is the time-dependent incremental component of pressure associated with the incompressibility constraint whose linearized measure is given by

$$\frac{\partial u_1}{\partial x_1} + \frac{\partial u_2}{\partial x_2} = 0. \tag{3}$$

In this paper, we focus on studying the effect of a vertical load, represented as a concentrated line force moving at a constant speed $v$, on the pre-stressed elastic half-space (see Fig. 1). Then, the boundary conditions on the surface $x_2 = 0$ are given in the following form

$$A_{2121}\frac{\partial u_1}{\partial x_2} + (A_{1221} + \bar{p})\frac{\partial u_2}{\partial x_1} = 0,$$

$$A_{1122}\frac{\partial u_1}{\partial x_1} + (A_{2222} + \bar{p})\frac{\partial u_2}{\partial x_2} - p_t = P_0\delta(x_1 - vt), \tag{4}$$

where $\bar{p} = A_{2121} - A_{1221} - \sigma_2$ is static pressure in the equilibrium state $B_e$, $\sigma_2$ is the normal Cauchy stress component, $\delta$ is the Dirac delta function, and $P_0$ is the amplitude.

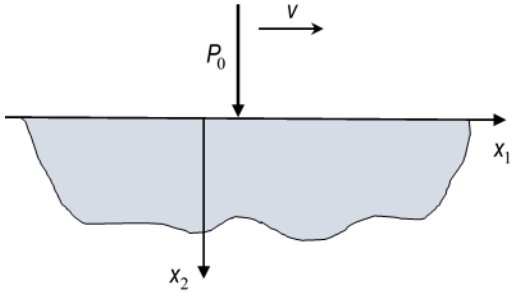


**Fig. 1.** Pre-stressed elastic half-space under the effect of a moving load

We consider the near-resonant regime, when the speed of the moving load is close to surface wave speed, thus the contribution of surface wave dominates over that of the bulk waves.

Introducing the auxiliary harmonic function $\psi_1$ (see (Khajiyeva et al., 2018) for details), the displacements may be expressed as

$$u_1(x_1, x_2, t) = \frac{\partial \psi_1(x_1, k_1 x_2, t)}{\partial x_2} + \vartheta\frac{\partial \psi_1(x_1, k_2 x_2, t)}{\partial x_2},$$

$$u_2(x_1, x_2, t) = -\frac{\partial \psi_1(x_1, k_1 x_2, t)}{\partial x_1} - \vartheta\frac{\partial \psi_1(x_1, k_2 x_2, t)}{\partial x_1}, \tag{5}$$

where $\vartheta = \frac{\gamma(k_1^2+1)-\sigma_2}{\gamma(k_2^2+1)-\sigma_2}$, and $k_1$, $k_2$ are related by

$$k_1^2 + k_2^2 = \frac{2\beta - \rho c_R^2}{\gamma}, \quad k_1^2 k_2^2 = \frac{\alpha - \rho c_R^2}{\gamma}, \tag{6}$$

with

$$\alpha = A_{1212}, \quad 2\beta = A_{1111} + A_{2222} - 2(A_{1122} + A_{1221}),$$

$$\gamma = A_{2121},$$

and $c_R$ denoting surface wave speed, being the solution of

$$\gamma(\alpha - \rho c_R^2) + (2\beta + 2\gamma - 2\sigma_2 - \rho c_R^2)\sqrt{\gamma(\alpha - \rho c_R^2)} = (\gamma - \sigma_2)^2,$$

see (Dowaikh and Ogden, 1990).

The approximate formulation of the original problem in elasticity (2)-(4) oriented towards the surface wave field has been developed in (Khajiyeva et al., 2018), reducing the vector problem in elasticity to a scalar problem for the elliptic equation in respect of the potential $\psi_1$. The methodology of the derivation relies on the slow-time perturbation procedure, extending the previous results for isotropic elasticity, see (Kaplunov and Prikazchikov, 2017). The resulting hyperbolic-elliptic model for surface wave field in a pre-stressed incompressible elastic half-space excited by the vertical surface loading $f_2 = f_2(x_1, t)$ is formulated in terms of the potential $\psi_1$ as elliptic equation

$$\frac{\partial^2 \psi_1}{\partial x_2^2} + k_1^2\frac{\partial^2 \psi_1}{\partial x_1^2} = 0, \tag{7}$$

subject to the boundary condition on the surface given by a hyperbolic equation (cf. formula (39) in (Khajiyeva et al., 2018))

$$\frac{\partial^2 \psi_1}{\partial x_1^2} - \frac{1}{c_R^2}\frac{\partial^2 \psi_1}{\partial t^2} = -\frac{2a_{11}f_2^*}{c_R(a_{21}b_1 - a_{11}b_2)} \quad \text{at } x_2 = 0, \tag{8}$$

where

$$a_{11} = \gamma(k_1^2 + 1) - \sigma_2, \quad a_{21} = k_1\left(2\beta - \rho c_R^2 - \sigma_2 - \gamma(k_1^2 - 1)\right),$$

$$f_2 = P_0\delta(x_1 - vt), \quad b_1 = \frac{2\rho c_R}{k_2^2 - k_1^2}\left(k_1^2 - 1 - \vartheta(k_2^2 - 1)\right),$$

$$b_2 = g_1 + \vartheta g_2,$$

$$g_j = \frac{\rho c_R(k_j^2 - 1)}{\gamma k_j(k_m^2 - k_j^2)}\left(2\beta - \rho c_R^2 - \sigma_2 + \gamma\left(1 - 3k_j^2\right)\right) - 2k_j\rho c_R,$$

$$j, m = 1,2; \ j \neq m,$$

and the asterisk denotes the Hilbert integral transform. Let us adapt this asymptotic formulation (7), (8) to the considered moving load problem.

## 3. EXPLICIT STEADY-STATE SOLUTION FOR THE NEAR-RESONANT REGIME

For the sake of convenience, the asymptotic model (7), (8) can be expressed in terms of the harmonic conjugate of $\psi_1$. The elliptic equation (7) becomes

$$\frac{\partial^2 \psi_1^*}{\partial x_2^2} + k_1^2\frac{\partial^2 \psi_1^*}{\partial x_1^2} = 0, \tag{9}$$

and the hyperbolic equation (8) is rewritten as

$$\frac{\partial^2\psi_1^*}{\partial x_1^2}-\frac{1}{c_R^2}\frac{\partial^2\psi_1^*}{\partial t^2}=P_1\delta(x_1-vt)\ \ \text{at}\ x_2=0, \tag{10}$$

where $P_1=\frac{2a_{11}P_0}{c_R(a_{21}b_1-a_{11}b_2)}$.

Now consider the steady-state regime and introduce a moving coordinate

$$\xi=x_1-vt. \tag{11}$$

Then, equation (10) takes the form

$$\left(1-\frac{v^2}{c_R^2}\right)\frac{\partial^2\psi_1^*}{\partial\xi^2}=P_1\delta(\xi). \tag{12}$$

On integrating the latter, we have

$$\frac{\partial\psi_1^*}{\partial\xi}=-\frac{c_R^2P_1}{v_-v_+}\left(H(\xi)-\frac{1}{2}\right), \tag{13}$$

where the constant of integration is chosen according to the symmetry rule as it cannot be determined by consideration of the steady-state regime (Kaplunov and Prikazchikov, 2017), and $v_\pm=v\pm c_R$.

Hence, restoring the solution into the interior, we obtain

$$\frac{\partial\psi_1^*(\xi,k_1x_2)}{\partial\xi}=-\frac{c_R^2P_1}{\pi v_-v_+}\tan^{-1}\frac{\xi}{k_1x_2}, \tag{14}$$

from which the harmonic conjugate function can be found as

$$\frac{\partial\psi_1(\xi,k_1x_2)}{\partial\xi}=\frac{c_R^2P_1}{2\pi v_-v_+}\ln(\xi^2+k_1^2x_2^2). \tag{15}$$

Thus, on substituting (14) and (15) into (5), the displacements $u_1$ and $u_2$ are given explicitly by

$$u_1=\frac{c_R^2P_1}{\pi v_-v_+}\left[k_1\tan^{-1}\frac{\xi}{k_1x_2}+\vartheta k_2\tan^{-1}\frac{\xi}{k_2x_2}\right],$$

$$u_2=-\frac{c_R^2P_1}{2\pi v_-v_+}[\ln(\xi^2+k_1^2x_2^2)+\vartheta\ln(\xi^2+k_2^2x_2^2)] \tag{16}$$

The resonant nature of surface wave speed is clearly observed from solutions (16).

## 4. TRANSIENT MOVING LOAD PROBLEM

Now let us consider a transient problem. Within this paper, we rely on the approach presented in (Kaplunov et al., 2010a), with the solution of the hyperbolic equation (10) written as a convolution of the right-hand side with the fundamental solution, namely

$$\psi_1^*(\xi,0,t)=\frac{c_RP_1}{2}\int_0^t\big(H(\xi+v_-r)-H(\xi+v_+r)\big)dr, \tag{17}$$

where $H$ is the Heaviside function.

The form of the integral in (17) motivates separate study of three regimes, including the sub-Rayleigh ($v<c_R$), super-Rayleigh ($v>c_R$) and the resonant one ($v=c_R$).

Introducing $\varphi=-\frac{2}{c_RP_1}\psi_1^*$ for convenience, we obtain for

a) sub-Rayleigh regime ($v<c_R$):

$$\varphi(\xi,0,t)=\begin{cases}\frac{\xi}{v_-}+t,\ \ 0\le\xi<-v_-t,\\ \frac{\xi}{v_+}+t,\ \ -v_+t<\xi<0,\\ \ \ 0,\ \ \text{otherwise}\end{cases} \tag{18}$$

b) super-Rayleigh regime ($v>c_R$):

$$\varphi(\xi,0,t)=\begin{cases}\xi\left(\frac{1}{v_+}-\frac{1}{v_-}\right),\ \ -v_-t\le\xi\le 0,\\ \frac{\xi}{v_+}+t,\ \ -v_+t<\xi<-v_-t,\\ \ \ 0,\ \ \text{otherwise}\end{cases} \tag{19}$$

c) resonant regime ($v=c_R$):

$$\varphi(\xi,0,t)=\begin{cases}\frac{\xi}{2c_R}+t,\ \ -2c_Rt\le\xi\le 0,\\ \ \ 0,\ \ \text{otherwise}\end{cases} \tag{20}$$

Now, once the solution has been found on the surface $x_2=0$ in the terms of the function $\varphi$, we can conduct the analysis with depth, i.e. restore the solution over the interior of the half-space $x_2>0$. Using the elliptic equation (9) and applying Poisson's formula, the potential $\psi_1^*$ is expressed as

$$\psi_1^*(\xi,k_1x_2,t)=\frac{1}{\pi}\int_{-\infty}^{+\infty}\frac{k_1x_2}{(r-\xi)^2+k_1^2x_2^2}\psi_1^*(r,0,t)dr. \tag{21}$$

Let us once again present the results in sequence for all three considered regimes.

### 4.1. Sub-Rayleigh regime

On substituting (18) into (21), after integration we get

$$\psi_1^*(\xi,k_1x_2,t)=\frac{c_RP_1}{2\pi}\left[\frac{h(\xi,k_1x_2,\xi_2)}{v_+}-\frac{h(\xi,k_1x_2,\xi_1)}{v_-}\right], \tag{22}$$

where

$$h(\xi,k_1x_2,\xi_i)=\frac{k_1x_2}{2}\ln\frac{(\xi-\xi_i)^2+k_1^2x_2^2}{\xi^2+k_1^2x_2^2}+\xi\tan^{-1}\frac{\xi}{k_1x_2}-(\xi-\xi_i)\tan^{-1}\frac{\xi-\xi_i}{k_1x_2}\ \ (i=1,2),$$

and

$$\xi_1=-v_-t,\ \ \xi_2=-v_+t.$$

Displacements (5) in terms of $\psi_1^*$ take the following form

$$u_1=-k_1\frac{\partial\psi_1^*(\xi,k_1x_2,t)}{\partial\xi}-\vartheta k_2\frac{\partial\psi_1^*(\xi,k_2x_2,t)}{\partial\xi},$$

$$u_2=-\frac{1}{k_1}\frac{\partial\psi_1^*(\xi,k_1x_2,t)}{\partial x_2}-\frac{\vartheta}{k_2}\frac{\partial\psi_1^*(\xi,k_2x_2,t)}{\partial x_2}. \tag{23}$$

Then, on substituting (22) into (23), the transient displacements are written explicitly as

$$u_1=\frac{c_R^2P_1}{\pi v_-v_+}\left[k_1\tan^{-1}\frac{\xi}{k_1x_2}+\vartheta\,k_2\tan^{-1}\frac{\xi}{k_2x_2}\right]+\frac{c_RP_1}{2\pi v_+}\left[k_1\tan^{-1}\frac{\xi-\xi_2}{k_1x_2}+\vartheta\,k_2\tan^{-1}\frac{\xi-\xi_2}{k_2x_2}\right]-\frac{c_RP_1}{2\pi v_-}\left[k_1\tan^{-1}\frac{\xi-\xi_1}{k_1x_2}+\vartheta\,k_2\tan^{-1}\frac{\xi-\xi_1}{k_2x_2}\right], \tag{24}$$

$$u_2=-\frac{c_RP_1}{4\pi v_+}\left[\ln\frac{(\xi-\xi_2)^2+k_1^2x_2^2}{\xi^2+k_1^2x_2^2}+\vartheta\ln\frac{(\xi-\xi_2)^2+k_2^2x_2^2}{\xi^2+k_2^2x_2^2}\right]+\frac{c_RP_1}{4\pi v_-}\left[\ln\frac{(\xi-\xi_1)^2+k_1^2x_2^2}{\xi^2+k_1^2x_2^2}+\vartheta\ln\frac{(\xi-\xi_1)^2+k_2^2x_2^2}{\xi^2+k_2^2x_2^2}\right]. \tag{25}$$

Represent equation (24) as

$$u_1=u_1^{st}(\xi,x_2)+u_1^{r0}, \tag{26}$$

where $u_1^{st}$ corresponds to the steady-state displacement (16$_1$), and

$$u_1^{r0}=\frac{c_RP_1v(k_1+\vartheta k_2)}{2v_-v_+} \tag{27}$$

is associated with the rigid body motion of the half-space, determined from analysis of the limiting behavior of displacements as $t\to\infty$.

Similarly, equation (25) can be reduced to

$$u_2 = u_2^{st}(\xi, x_2) + u_2^{r0} + u_2^{r1}\ln t, \tag{28}$$

where $u_2^{st}$ corresponds to formula (16$_2$), and

$$u_2^{r0} = -\frac{c_R P_1(1+\vartheta)}{2\pi}\left[\frac{\ln v_+}{v_+} - \frac{\ln|v_-|}{v_-}\right],$$

$$u_2^{r1} = \frac{{c_R}^2 P_1(1+\vartheta)}{\pi v_- v_+}. \tag{29}$$

Thus, explicit expressions for rigid body motion have been obtained. It also follows from (29) that the vertical rigid body motion had a logarithmic growth in time, which is consistent with the previous results for isotropic elasticity in (Kaplunov et al., 2010a).

### 4.2. Super-Rayleigh regime

On substituting (19) into (21) and performing straightforward manipulations, we deduce

$$\psi_1^*(\xi, k_1x_2, t) = -\frac{c_R P_1}{2\pi}\left[\frac{2c_R}{v_- v_+}\left(\frac{k_1x_2}{2}\ln\frac{(\xi-\xi_1)^2+k_1^2x_2^2}{\xi^2+k_1^2x_2^2} + \right.\right.$$
$$\left.\xi\tan^{-1}\frac{\xi}{k_1x_2} - \xi\tan^{-1}\frac{\xi-\xi_1}{k_1x_2}\right) - \frac{1}{c_R+v}\left(\frac{k_1x_2}{2}\ln\frac{(\xi-\xi_2)^2+k_1^2x_2^2}{(\xi-\xi_1)^2+k_1^2x_2^2} + (\xi -$$
$$\left.\left.\xi_2)\tan^{-1}\frac{\xi-\xi_1}{k_1x_2} - (\xi-\xi_2)\tan^{-1}\frac{\xi-\xi_2}{k_1x_2}\right)\right]. \tag{30}$$

Then, from (23), the displacements $u_1$ and $u_2$ are obtained, coinciding with those for the sub-Rayleigh regime, namely (24) and (25). Study of the limiting behavior of both displacements also gives the same structure (26)-(29), except for $u_1^{r0}$ that now is determined by

$$u_1^{r0} = -\frac{c_R^2 P_1(k_1+\vartheta k_2)}{2v_- v_+}. \tag{31}$$

### 4.3. Resonant regime

Here we study the case when the speed of the moving load coincides with the surface wave speed. Taking into account (20), the potential $\psi_1^*$ is found as

$$\psi_1^*(\xi, k_1x_2, t) = \frac{P_1}{4\pi}\left[\frac{k_1x_2}{2}\ln\frac{(\xi+2c_Rt)^2+k_1^2x_2^2}{\xi^2+k_1^2x_2^2} + (\xi +\right.$$
$$\left.2c_Rt)\left(\tan^{-1}\frac{\xi}{k_1x_2} - \tan^{-1}\frac{\xi+2c_Rt}{k_1x_2}\right)\right]. \tag{32}$$

Substituting (32) into (23), we have

$$u_1 = -\frac{c_R P_1 x_2 t}{2\pi}\left[\frac{k_1^2}{\xi^2+k_1^2x_2^2} + \frac{\vartheta k_2^2}{\xi^2+k_2^2x_2^2}\right] - \frac{P_1k_1}{4\pi}\left[\tan^{-1}\frac{\xi}{k_1x_2} -\right.$$
$$\left.\tan^{-1}\frac{\xi+2c_Rt}{k_1x_2}\right] - \frac{P_1\vartheta k_2}{4\pi}\left[\tan^{-1}\frac{\xi}{k_2x_2} - \tan^{-1}\frac{\xi+2c_Rt}{k_2x_2}\right], \tag{33}$$

$$u_2 = \frac{c_R P_1 \xi t}{2\pi}\left[\frac{1}{\xi^2+k_1^2x_2^2} + \frac{\vartheta}{\xi^2+k_2^2x_2^2}\right] - \frac{P_1}{8\pi}\left[\ln\frac{(\xi+2c_Rt)^2+k_1^2x_2^2}{\xi^2+k_1^2x_2^2} +\right.$$
$$\left.\vartheta\ln\frac{(\xi+2c_Rt)^2+k_2^2x_2^2}{\xi^2+k_2^2x_2^2}\right]. \tag{34}$$

The limiting behavior of displacements as $t \to \infty$ for resonant case gives

$$u_1 = -\frac{c_R P_1 x_2 t}{2\pi}\left[\frac{k_1^2}{\xi^2+k_1^2x_2^2} + \frac{\vartheta k_2^2}{\xi^2+k_2^2x_2^2}\right], \tag{35}$$

and

$$u_2 = \frac{c_R P_1 \xi t}{2\pi}\left[\frac{1}{\xi^2+k_1^2x_2^2} + \frac{\vartheta}{\xi^2+k_2^2x_2^2}\right] - \frac{P_1(1+\vartheta)}{4\pi}\ln(2c_Rt). \tag{36}$$

## 5. NUMERICAL ILLUSTRATIONS

First, let us illustrate the obtained steady-state solution (16). Three forms of the strain-energy function are considered below, namely the neo-Hookean, Gent, and Gent-Gent models, which are typically used for modelling rubber-like materials.

The well-known neo-Hookean strain-energy function is written as

$$W = \frac{\mu}{2}(I_1 - 3), \tag{37}$$

where $\mu$ is the ground-state shear modulus, and $I_1$ is given by

$$I_1 = \lambda_1^2 + \lambda_2^2 + \lambda_3^2, \tag{38}$$

where $\lambda_i$ $\left(i = \overline{1,3}\right)$ are the principal stretches of the underlying deformation, related by an incompressibility condition $\lambda_1\lambda_2\lambda_3 = 1$ (see (Dowaikh and Ogden, 1990) for more details).

Consider also extensions of the neo-Hookean model, including the Gent strain-energy function (Gent, 1996)

$$W = -\frac{\mu}{2}J_m\ln\left(1 - \frac{I_1-3}{J_m}\right), \tag{39}$$

where $J_m$ is a material constant characterizing material extensibility and the shear modulus $\mu = \mu_0 + \frac{2C_2}{3}$ with $C_2$ denoting the material constant, along with its more advanced version usually referred to as the Gent-Gent material model (Pucci and Saccomandi, 2002) defined by

$$W = -\frac{\mu_0}{2}J_m\ln\left(1 - \frac{I_1-3}{J_m}\right) + C_2\ln\left(\frac{I_2}{3}\right), \tag{40}$$

where $I_1$ is given by (38), and $I_2 = \lambda_1^{-2} + \lambda_2^{-2} + \lambda_3^{-2}$, see also a recent contribution by (Zhou et al., 2018).

Figs. 2, 3 demonstrate the computation results for different forms of the strain-energy function at the depth $x_2 = 0.5$. The system parameters are chosen as follows: $\mu_0 = 0.2853$ MPa, $C_2 = 0.1898$ MPa, $J_m = 88.43$ (according to (Zhou et al., 2018)), $\rho = 1522\,\mathrm{kg/m^3}$, $v = 0.8\,c_R$, $P_0 = 1$, $\lambda_1 = 1.25$, $\lambda_2 = \lambda_1^{-1}, \lambda_3 = 1$. It is also assumed that a parameter $Z = 0$, which is used for calculating the normal Cauchy stress $\sigma_2$ (Dowaikh and Ogden, 1990),

$$\sigma_2 = \gamma - \sqrt{\gamma\alpha} + Z\sqrt{2\sqrt{\gamma\alpha}(\beta + \sqrt{\gamma\alpha})}, \quad -1 \le Z \le 1, \tag{41}$$

so the surface wave has a non-zero velocity and is localized.

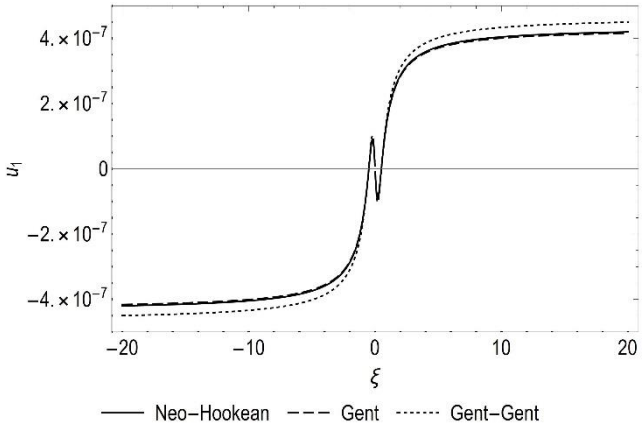


**Fig. 2.** Horizontal displacement $u_1$ for the neo-Hookean, Gent and Gent-Gent material models

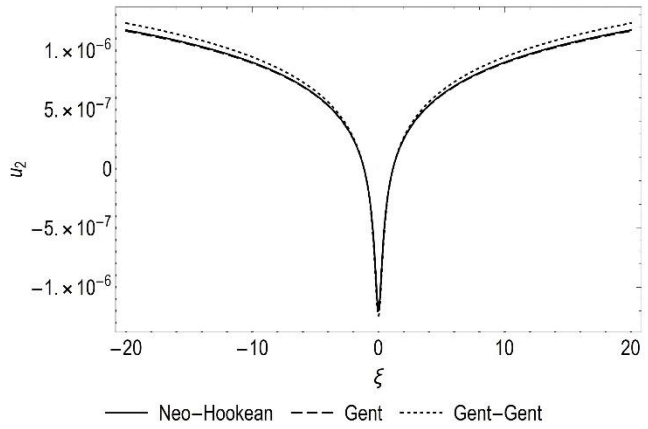


**Fig. 3.** Vertical displacement $u_2$ for the neo-Hookean, Gent and Gent-Gent material models

As can be seen from Figs. 2, 3, the neo-Hookean and Gent material models give almost identical results for both displacements $u_1$ and $u_2$, whereas using the Gent-Gent model results in higher values of the displacement amplitudes with increasing $\xi$. In what follows, we use the Gent-Gent model since it seemingly provides a better agreement with experimental data, as demonstrated in (Zhou et al., 2018).

Variation of the amplitude of the surface displacements $u_1$ and $u_2$ on the moving coordinate is illustrated in Figs. 4, 5 for several values of the transverse variable $x_2$.

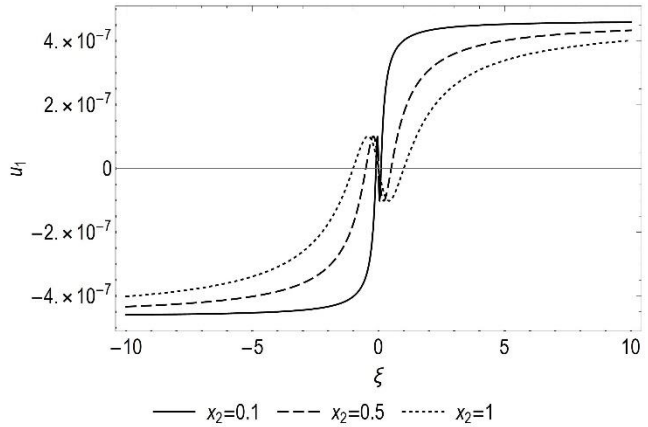


**Fig. 4.** Dependence of displacement $u_1$ on the moving coordinate $\xi$ for different values of $x_2$

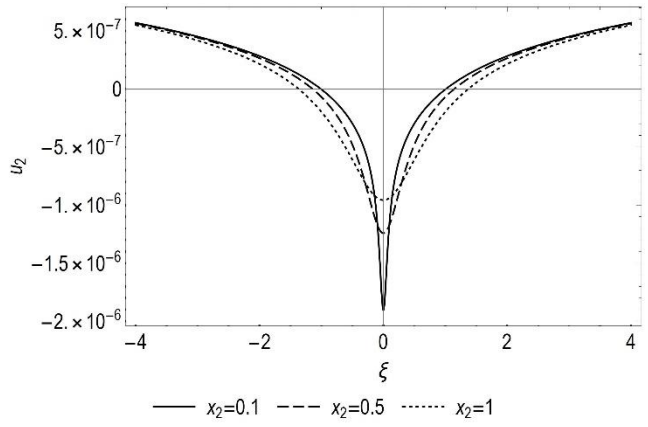


**Fig. 5.** Dependence of displacement $u_2$ on the moving coordinate $\xi$ for different values of $x_2$

Predictably, the obtained graphs (Figs. 4, 5) indicate smoothening of displacements profiles under the moving load with increase in depth.

To present the numerical results for the transient moving load problem, the Gent-Gent model (40) is utilized, for the same material parameters as before. The speed of the moving load for various regimes is taken as $v = 0.8\ c_R$, $v = 1.2\ c_R$ and $v = c_R$ for the sub-Rayleigh, super-Rayleigh, and resonant regimes, respectively (Figs. 6-11).

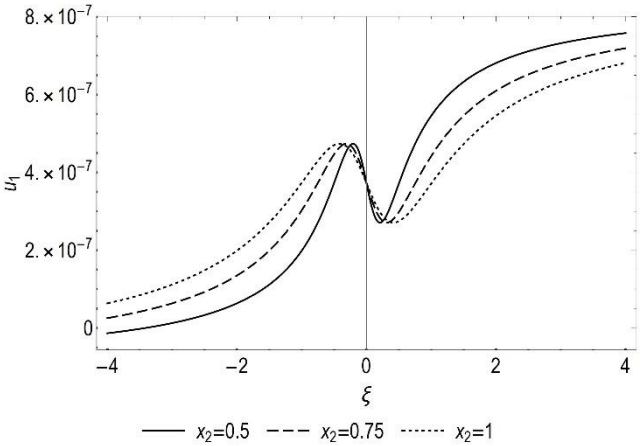


**Fig. 6.** The sub-Rayleigh transient displacement $u_1$ for different values of $x_2$

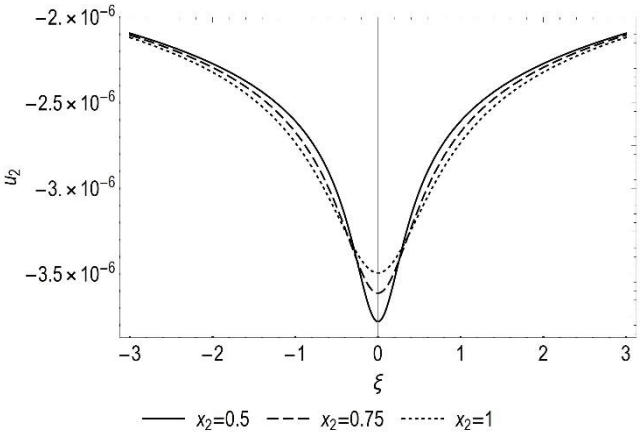


**Fig. 7.** The sub-Rayleigh transient displacement $u_2$ for different values of $x_2$

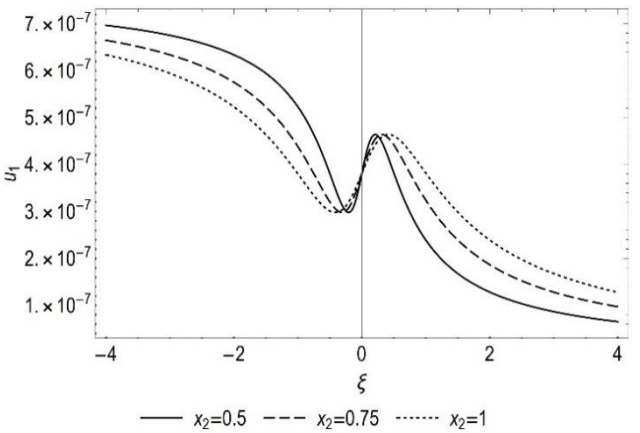


**Fig. 8.** The super-Rayleigh transient displacement $u_1$ for different values of $x_2$

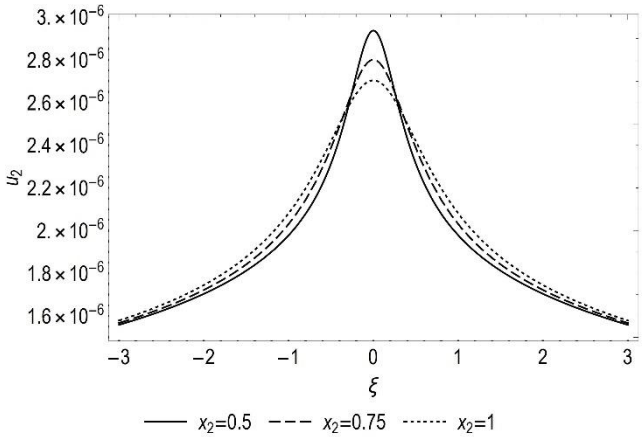


**Fig. 9.** The super-Rayleigh transient displacement $u_2$ for different values of $x_2$

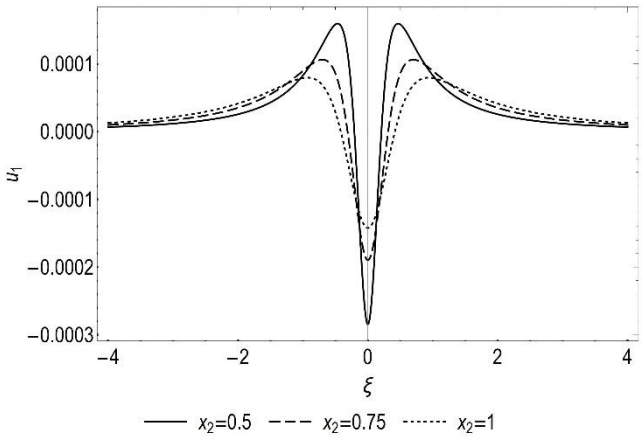


**Fig. 10.** The resonant transient displacement $u_1$ for different values of $x_2$

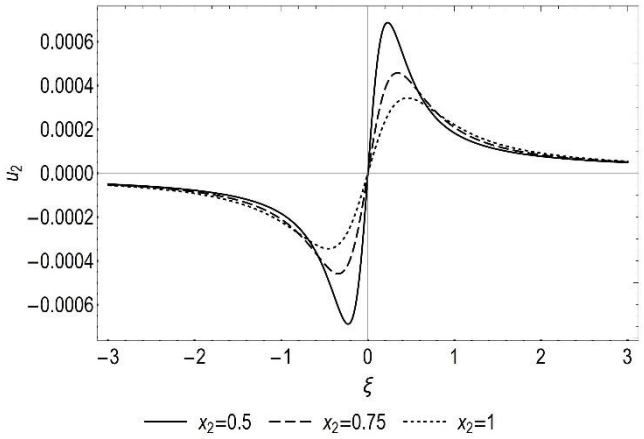


**Fig. 11.** The resonant transient displacement $u_2$ for different values of $x_2$

Figs. 6, 7 demonstrate the sub-Rayleigh transient displacements $u_1$ and $u_2$, Figs. 8, 9 – the super-Rayleigh transient displacements, see (24), (25), and Figs. 10, 11 correspond to the resonant transient displacements (33), (34), depending on the values of the vertical coordinate $x_2$.

It is emphasized that the obtained shapes of displacements are typical for a broad range of deformations, with qualitatively similar behaviour occurring for the non-deformed linear isotropic case as well, when $\lambda_1 = \lambda_2 = \lambda_3 = 1$.

It should be noted that the accuracy of the approximate results within the model has been discussed in (Kaplunov and Prikazchikov, 2017; Sect. 4.3.1), where it was shown that for a wide class of loads the asymptotic formulation captures the contribution of the Rayleigh poles. Moreover, in case of transient problem, as shown in (Kaplunov et al., 2010a), the near-resonant solution is valid for large times when the effect of the body waves becomes negligible. Moreover, comparison of exact and approximate solutions revealed a wide range of speeds in which the approximation performs at a reasonable accuracy (Fig. 8 of the cited paper).

## 6. CONCLUSION

The near-resonant regimes of the steady-state moving load problem on a pre-stressed, incompressible elastic half-space have been studied. Implementation of the hyperbolic-elliptic model for surface wave allowed explicit solutions for the displacement components. Illustrations in Figs. 2 and 3 are revealing some possible similarities between the neo-Hookean, Gent, and Gent-Gent material models. The consideration has then been extended to transient problem, allowing an elegant approximate solution in terms of elementary functions, which makes it convenient for further analysis, including the limiting behavior for large time, providing explicit results for the components of rigid body motion.

Various extensions of the approach include derivation of 3D asymptotic models in pre-stressed media. Although straightforward explicit approach could be cumbersome algebraically, there is a chance of more elegant representation though Stroh formalism, in line with results reported recently in (Fu et al., 2020). It is worth noting that adding vertical inhomogeneity will lead to smoothing of surface discontinuities, for more details see (Erbaş et al., 2017). Finally, we note that it is also possible to extend the methodology to composite models for elastic layers (Erbaş et al., 2018; Erbaş et al., 2019), as well as to consider the dynamics of pre-stressed half-space with cavities (Alekseeva and Ukrainets, 2009) and crack propagation (Mishuris et al., 2012; Gourgiotis and Piccolroaz, 2014).

## REFERENCES

1. **Alekseeva L.A., Ukrainets V.N.** (2009), Dynamics of an elastic half-space with a reinforced cylindrical cavity under moving loads, *Int. Appl. Mech.*, 45(9), 981-990.
2. **Bratov V.** (2011), Incubation time fracture criterion for FEM simulations, *Acta Mech. Sin.*, 27(4), 541.
3. **Cao Y., Xia H., Li Z.** (2012), A semi-analytical/FEM model for predicting ground vibrations induced by high-speed train through continuous girder bridge, *J. Mech. Sci. Technol.*, 26, 2485-2496.
4. **Cole J., Huth J.** (1958), Stresses produced in a half plane by moving loads, *J. Appl. Mech.*, 25, 433-436.
5. **van Dalen K.N., Tsouvalas A., Metrikine A.V., Hoving J.S.** (2015), Transition radiation excited by a surface load that moves over the interface of two elastic layers, *Int. J. Solids Struct.*, 73, 99-112.
6. **Dimitrovová Z.** (2017), Analysis of the critical velocity of a load moving on a beam supported by a finite depth foundation, *Int. J. Solids Struct.,* 122, 128-147
7. **Dowaikh M.A., Ogden R.W.** (1990), On surface waves and deformations in a pre-stressed incompressible elastic solid, *IMA J. Appl. Math.*, 44, 261-284.
8. **Ege N., Şahin O., Erbaş B.** (2017), Response of a 3D elastic half-space to a distributed moving load, *Hacet J. Math. Stat.*, 46(5), 817-

828.
9. **Ege N., Erbaş B., Kaplunov J., Wootton P.** (2018), Approximate analysis of surface wave-structure interaction, *J. Mech. Mater. Struct.*, 13(3), 297-309.
10. **Erbaş B., Kaplunov J., Prikazchikov D.A., Şahin O.** (2017), The near-resonant regimes of a moving load in a three-dimensional problem for a coated elastic half-space, *Math. Mech. Solids*, 22(1), 89–100.
11. **Erbaş B., Kaplunov J., Nolde E., Palsü M.** (2018), Composite wave models for elastic plates, *P. Roy. Soc. A-Math. Phy.*, 474(2214), 1-16.
12. **Erbaş B., Kaplunov J., Palsü M.** (2019), A composite hyperbolic equation for plate extension, *Mech. Res. Commun.*, 99, 64-67.
13. **Fryba L.** (1999), *Vibration of solids and structures under moving loads*, 3rd ed, Thomas Telford, London.
14. **Fu Y., Kaplunov J., Prikazchikov D.** (2020), Reduced model for the surface dynamics of a generally anisotropic elastic half-space, *P. Roy. Soc. A-Math. Phy.*, 476(2234), 1-19.
15. **Gakenheimer D.C., Miklowitz J.** (1969), Transient excitation of an elastic half space by a point load traveling on the surface, *J. Appl. Mech.*, 36(3), 505-515.
16. **Gent A.N.** (1996), A new constitutive relation for rubber, *Rubber Chem. Technol.*, 69(1), 59-61.
17. **Goldstein R.V.** (1965), Rayleigh waves and resonance phenomena in elastic bodies, *J. Appl. Math. Mech. (PMM)*, 29(3), 516-525.
18. **Gourgiotis P.A., Piccolroaz A.** (2014), Steady-state propagation of a mode II crack in couple stress elasticity, Int. J. Fract., 188(2), 119-145.
19. **de Hoop A.T.** (2002), The moving-load problem in soil dynamics – the vertical displacement approximation, *Wave Motion*, 36(4), 335-346.
20. **Kaplunov J., Nolde E., Prikazchikov D.A.** (2010a), A revisit to the moving load problem using an asymptotic model for the Rayleigh wave, *Wave Motion*, 47, 440-451.
21. **Kaplunov J., Voloshin V., Rawlins A.D.** (2010b), Uniform asymptotic behaviour of integrals of Bessel functions with a large parameter in the argument, *Quart. J. Mech. Appl. Math.*, 63(1), 57-72.
22. **Kaplunov J., Prikazchikov D.A., Erbaş B., Şahin O.** (2013), On a 3D moving load problem for an elastic half space, *Wave Motion*, 50(8), 1229-1238.
23. **Kaplunov J., Prikazchikov D.A.** (2017), Asymptotic theory for Rayleigh and Rayleigh-type waves, *Adv. Appl. Mech.*, 50, 1-106.
24. **Kaplunov J., Prikazchikov D., Sultanova L.** (2019), Rayleigh-type waves on a coated elastic half-space with a clamped surface, *Phil. Trans. Roy. Soc. A*, 377(2156), 1-15.
25. **Khajiyeva L.A., Prikazchikov D.A., Prikazchikova L.A.** (2018), Hyperbolic-elliptic model for surface wave in a pre-stressed incompressible elastic half-space, *Mech. Res. Commun.*, 92, 49-53.
26. **Krylov V.V.** (1996), Vibrational impact of high-speed trains. I. Effect of track dynamics, *J. Acoust. Soc. Am.*, 100(5), 3121-3134.
27. **Kumar R., Vohra R.** (2020), Steady state response due to moving load in thermoelastic material with double porosity, *Mater. Phys. Mech.*, 44(2), 172-185.
28. **Lefeuve-Mesgouez G., Le Houédec D., Peplow A.T.** (2000), Ground vibration in the vicinity of a high-speed moving harmonic strip load, *J. Sound Vib.*, 231(5), 1289-1309.
29. **Lu T., Metrikine A.V., Steenbergen M.J.M.M.** (2020), The equivalent dynamic stiffness of a visco-elastic half-space in interaction with a periodically supported beam under a moving load, *Europ. J. Mech.-A/Solids*, 84, 104065.
30. **Mishuris G., Piccolroaz A., Radi E.** (2012), Steady-state propagation of a Mode III crack in couple stress elastic materials, *Int. J. Eng. Sci.*, 61, 112-128.
31. **Ogden R.W.** (1984), *Non-linear elastic deformations*, Dover, New York.
32. **Payton R.G.** (1967), Transient motion of an elastic half-space due to a moving surface line load, *Int. J. Eng. Sci.*, 5(1), 49-79.
33. **Pucci E., Saccomandi G.** (2002), A note on the Gent model for rubber-like materials, *Rubber Chem. Technol.*, 75(5), 839-852.
34. **Smirnov V., Petrov Yu.V., Bratov V.** (2012), Incubation time approach in rock fracture dynamics, *Sci. China Phys., Mech. Astr.*, 55(1), 78-85.
35. **Sun Z., Kasbergen C., Skarpas A., Anupam K., van Dalen K.N., Erkens S.M.** (2019), Dynamic analysis of layered systems under a moving harmonic rectangular load based on the spectral element method, *Int. J. Solids Struct.*, 180, 45-61.
36. **Wang F., Han X., Ding T.** (2021), An anisotropic layered poroelastic half-space subjected to a moving point load, *Soil Dyn. Earth. Eng.*, 140, 106427.
37. **Wang Y., Zhou A., Fu T., Zhang W.** (2020), Transient response of a sandwich beam with functionally graded porous core traversed by a non-uniformly distributed moving mass, *Int. J. Mech. Mater. Design*, 16(3), 519-540.
38. **Wootton P.T., Kaplunov J., Colquitt D.J.** (2019), An asymptotic hyperbolic-elliptic model for flexural-seismic metasurfaces, *P. Roy. Soc. A-Math. Phy.*, 475(2227), 1-18.
39. **Wootton P.T., Kaplunov J., Prikazchikov D.** (2020), A second-order asymptotic model for Rayleigh waves on a linearly elastic half plane, *IMA J. Appl. Math.*, 85, 113-131.
40. **Zhou L., Wang S., Li L., Fu Y.** (2018), An evaluation of the Gent and Gent-Gent material models using inflation of a plane membrane, *Int. J. Mech. Sci.*, 146-147, 39-48.

AKK and AKK acknowledge support by the Ministry of Science and Education of the Republic of Kazakhstan (Grant No. AP05132743, 2018-2020). DP was supported by the Russian Science Foundation, Grant No. 20-11-20133 in the part on “Explicit steady-state solution for the near-resonant regime”.